Research Article

Haiyun Wang, Xiaofeng Peng, Hao Zhang, Lin Liu*, Yahong Chen*, Fei Wang* and Yangjian Cai*

Experimental synthesis of partially coherent beam with controllable twist phase and measuring its orbital angular momentum

https://doi.org/10.1515/nanoph-2021-0432
Received August 8, 2021; accepted September 15, 2021; published online September 29, 2021

Abstract: Twist phase is a nontrivial second-order phase that only exists in a partially coherent beam. Such twist phase endows the partially coherent beam with orbital angular momentum (OAM) and has unique applications such as in super-resolution imaging. However, the manipulation and the detection of the twist phase are still far from easy tasks in experiment. In this work, we present a flexible approach to generate a famous class of twisted Gaussian Schell-model (TGSM) beam with controllable twist phase by the superposition of the complex field realizations using a single phase-only spatial light modulator. The precise control of the amplitude and phase of the field realizations allows one to manipulate the strength of the twist phase easily. In addition, we show that the twist factor, a key factor that determines the strength of twist phase and the amount of OAM, can be measured by extracting the real part of the complex degree of coherence of the TGSM beam. The experiment is carried out with the help of the generalized Hanbury Brown and Twiss experiment as the generated TGSM beam obeys Gaussian statistics. The flexible control and detection of the twist phase are expected to find applications in coherence and OAM-based ghost imaging.

***Corresponding authors: Lin Liu, Yahong Chen, Fei Wang and Yangjian Cai,** School of Physical Science and Technology, Soochow University, Suzhou 215006, China, E-mail: liulin@suda.edu.cn (L. Liu), yahongchen@suda.edu.cn (Y. Chen), fwang@suda.edu.cn (F. Wang), yangjiancai@suda.edu.cn (Y. Cai). https://orcid.org/0000-0003-3440-7709
Haiyun Wang and Hao Zhang, School of Physical Science and Technology, Soochow University, Suzhou 215006, China. https://orcid.org/0000-0001-6514-9090 (H. Zhang)
Xiaofeng Peng, School of Physics and Electronics, Shandong Provincial Engineering and Technical Center of Light Manipulations & Shandong Provincial Key Laboratory of Optics and Photonic Devices, Shandong Normal University, Jinan 250014, China

Keywords: optical coherence; orbital angular momentum; partially coherent beam; twist phase.

1 Introduction

Over the past three decades, light beams carrying orbital angular momentum (OAM) have been widely studied owing to their unique properties and diverse applications in optical tweezers, optical communications, nonlinear optics, and so on [1, 2]. Perhaps, the most known light beam carrying OAM is the vortex beam [3, 4]. Such beam possesses helical phase front i.e., $\exp(il\varphi)$, where l is the topological charge and φ is the azimuthal angle in polar coordinate [5]. In 1992, Allen and coauthors found that the vortex beam has a well-defined OAM, equivalent to $l\hbar$ per photon (l is an integer number), where $\hbar$ is the reduced Plank constant. This general result opens a new chapter in modern optics, i.e., singular optics [6]. The vortex beams and optical vortices can be generated and manipulated by various methods including the in-cavity and out-cavity approaches with the use of macroscopic and microstructural elements [3, 7–9]. Meanwhile, many approaches for the determination of the topological charge l have been proposed, such as with the slit interference [10–12], prescribed aperture diffraction [13], special diffraction gratings [14], coordinate transformation [15], mode conversion [16], and astigmatic transformation [17]. The generation and measurement of the vortex beam endowed with partial coherence have also been studied extensively [18–21]. Besides the vortex phase, astigmatic phase is another phase that could induce OAM [22, 23]. An elliptical Gaussian beam passing through a cylindrical lens could generate such astigmatic phase. The advantage of astigmatic phase is that it could produce very high OAM, e.g., up to $10,000\hbar$ per photon.

Twist phase is another nontrivial phase that could induce the light beams carrying the OAM [24, 25]. Different from the vortex and astigmatic phases, the twist phase is a *second-order* phase that depends on two spatial points and

cannot be separated with respect to two positions. Thus, the twist phase exists only in a partially coherent light and is encoded within the second-order coherence function. Compared with the fully coherent light, the partially coherent light has found advantages in many applications [26–29]. The expression for the twist phase is $\exp[-i\mu_0(x_1y_2 - x_2y_1)]$, where μ_0 is the twist factor, related to the amount of OAM carried by each photon and (x_1, y_1), (x_2, y_2) are two arbitrary position vectors in the beam transverse plane. The twist factor is bounded by $|\mu_0| \le \delta_0^{-2}$, where δ_0 is the transverse spatial coherence width of the light beam. We can find when the beam becomes fully coherent, i.e., δ_0 tends to infinity, $\mu_0 = 0$, and the twist phase disappears. Since Simon et al. introduced the twist phase in a Gaussian Schell-model beam, which is named the twisted Gaussian Schell-model (TGSM) beam, the propagation of the TGSM beam in paraxial optical systems, dispersive media, and uniaxial crystal has been well explored theoretically [30–34]. The OAM flux density and its interaction with vortex phase were also studied in detail [35]. Recently, the studies of the conditions for embedding the twist phase in other kinds of partially coherent beams and devising new kind of twisted beams have paid considerable attention [36–40]. The TGSM beam has found potential applications in super-resolution imaging, optical trapping, free-space optical communications, and beam self reconstruction enhancement [41–44]. However, the experimental generation of the TGSM beam with controllable twist factor is far from an easy task. To the best of our knowledge, there are only a few reports to generate the TGSM beam experimentally. One way is to a transform anisotropic GSM beam to the TGSM beam by using six or three cylindrical lenses system [45, 46]. However, this approach is difficult to modulate the twist factor. Another method proposed recently is the incoherent superposition of the continuous coherent modes [47, 48]. In that method, the generated twisted beam does not obey Gaussian statistics as the modes are not randomly fluctuating. Thus, it is restricted in particular applications where the Gaussian statistics is required, e.g., in ghost imaging [49, 50]. In addition, the experimental measurement of the twist factor of the TGSM beam is still a tricky challenge as the TGSM beam has the very weak spatial coherence and therefore the traditional interferometric methods cannot be used. As far as we know, there is no report on the experimental measurement of the twist phase.

In this work, we introduce an efficient way to generate the TGSM beam with controllable twist phase with the aid of a single phase-only spatial light modulator (SLM). The methodology is based on the superposition of the random modes generated by the stochastic complex transmittance screens [51]. Thus, the generated TGSM beam obeys Gaussian statistics. Moreover, we show that the twist factor can be quantitatively measured from extracting the real part of the two-point complex degree of coherence (DOC) of the twisted source. A proof-of-principle experiment is carried out to determine the twist phase of the generated TGSM beam with the help of the generalized Hanbury Brown and Twiss effect [52]. Our results open a new avenue for manipulating the second-order phase and OAM of the partially coherent light and may find novel applications in optical trapping, imaging, and optical communications.

2 Theory

The second-order statistical properties of a TGSM beam, propagating along z-axis, is characterized by a two-point cross-spectral density (CSD) function in space-frequency domain [24]

$$W(\mathbf{r_1}, \mathbf{r_2}) = \langle E^*(\mathbf{r_1}) E(\mathbf{r_2}) \rangle = \exp\left[-\frac{1}{4\sigma_0^2}(\mathbf{r_1^2} + \mathbf{r_2^2}) \right] \mu(\mathbf{r_1}, \mathbf{r_2}), \quad (1)$$

with

$$\mu(\mathbf{r_1}, \mathbf{r_2}) = \exp\left[-\frac{1}{2\delta_0^2}(\mathbf{r_1} - \mathbf{r_2})^2 \right] \exp[-i\mu_0(\mathbf{r_1} \times \mathbf{r_2})_\perp]. \quad (2)$$

Above $\mu(\mathbf{r_1}, \mathbf{r_2})$ is the complex DOC function, $\mathbf{r_1} = (x_1, y_1)$ and $\mathbf{r_2} = (x_2, y_2)$ are two position vectors in the source plane ($z = 0$), $E(\mathbf{r})$ denotes the electric field realization, the asterisk and the angular brackets stand for the complex conjugate and ensemble average over the source fluctuations, respectively. σ_0 and δ_0 are the beam width and the spatial coherence width, respectively. The subscript $\perp$ in Eq. (2) denotes the component of cross-product orthogonal to the propagation axis. μ_0 is a twist factor, a measure of the strength of the twist phase. The magnitude of μ_0 is bounded by the inequality $|\mu_0| \le \delta_0^{-2}$, which ensures the nonnegative definiteness of the CSD function. When $\mathbf{r} = \mathbf{r_1} = \mathbf{r_2}$, the CSD function reduces to the average intensity of the TGSM beam, i.e., $S(\mathbf{r}) = W(\mathbf{r}, \mathbf{r}) = \langle I(\mathbf{r}) \rangle$.

In order to synthesize the TGSM source experimentally, the DOC function can be written as the following alternative integral form

$$\mu(\mathbf{r}_1,\mathbf{r}_2)=\exp[-\alpha(\mathbf{r}_1^2+\mathbf{r}_2^2)\mu_0^2/2]\int\int p(\mathbf{v})H^*(\mathbf{r}_1,\mathbf{v})H(\mathbf{r}_2,\mathbf{v})d^2\mathbf{v}. \quad (3)$$

The function $p(\mathbf{v})$ and $H(\mathbf{r},\mathbf{v})$ take the form

$$p(\mathbf{v})=\alpha\exp(-\alpha\mathbf{v}^2)/\pi, \quad (4)$$

$$H(\mathbf{r},\mathbf{v})=\exp[\alpha\mu_0(xv_y-yv_x)]\exp[-i(xv_x+yv_y)]. \quad (5)$$

The parameters α, μ_0, and δ_0 satisfy the relation: $(2\delta_0^2)^{-1}=\alpha\mu_0^2/4+(4\alpha)^{-1}$. To produce the random fields whose correlation function have the complex DOC shown in Eq. (3), we let H be a realization of an optical field parameterized by random vector $\mathbf{v}=(v_x, v_y)$, and $p(\mathbf{v})$ interprets as the joint probability function of $\mathbf{v}$. Now, let us consider a form of stochastic optical field generated by a deterministic field $\tau(\mathbf{r})$ passing through a complex random screen $T(\mathbf{r})$, given by $E(\mathbf{r})=\tau(\mathbf{r})T(\mathbf{r})$. Taking the second-order statistic of the stochastic field, one obtains the CSD function.

$$W(\mathbf{r}_1,\mathbf{r}_2)=\tau^*(\mathbf{r}_1)\tau(\mathbf{r}_2)\langle T^*(\mathbf{r}_1)T(\mathbf{r}_2)\rangle. \quad (6)$$

Compared Eq. (6) to Eqs. (1) and (3), one could establish the bridge between the complex DOC and the complex random screens, which is

$$\langle T^*(\mathbf{r}_1)T(\mathbf{r}_2)\rangle=\int\int p(\mathbf{v})H^*(\mathbf{r}_1,\mathbf{v})H(\mathbf{r}_2,\mathbf{v})d^2\mathbf{v}, \quad (7)$$

and $\tau(\mathbf{r})=\exp\{-[(4\sigma_0^2)^{-1}+\alpha\mu_0^2/2]\mathbf{r}^2\}$. Following from the analysis in Ref. [51], the complex random screen $T(\mathbf{r})$ can be evaluated from the following integral by changing the variable $\mathbf{v}=2\pi\mathbf{f}$, i.e.,

$$T(\mathbf{r})=\sqrt{2\pi\alpha}\int\int R(\mathbf{f})[2\pi^2p(2\pi\mathbf{f})]^{1/2}H(\mathbf{r},2\pi\mathbf{f})d^2\mathbf{f}, \quad (8)$$

where $R(\mathbf{f})$ is the circular complex Gaussian random numbers with zero mean and unit variance. Eq. (8) can be evaluated numerically by means of the fast Fourier transform (FFT) algorithm. The procedure for the computing the single realization, say $T_n(\mathbf{r})$ ($n=1, 2, 3, \ldots$) of the stochastic field is as follows: The first exponential function in H function is evaluated at a desired location (x_i, y_j), then performing the two-dimensional FFT of Eq. (8). The result of the FFT at the location (x_i, y_j) is the true value of the screen $T_n(\mathbf{r})$. The above procedure is repeated for all (x_i, y_j) in the transverse plane. Finally, the obtained screen $T_n(\mathbf{r})$ is multiplied by a Gaussian function $\tau(\mathbf{r})$. Figure 1(a) and (b) show the simulation results of the distribution of the intensity and the phase of one realization of random electric field $E(\mathbf{r})$. The parameters are chosen to be $\sigma_0=1.6$ mm, $\delta_0=0.4$ mm, and $\mu_0=6.25$ mm^{-2}. Obviously, the amplitude and phase fluctuate randomly in space.

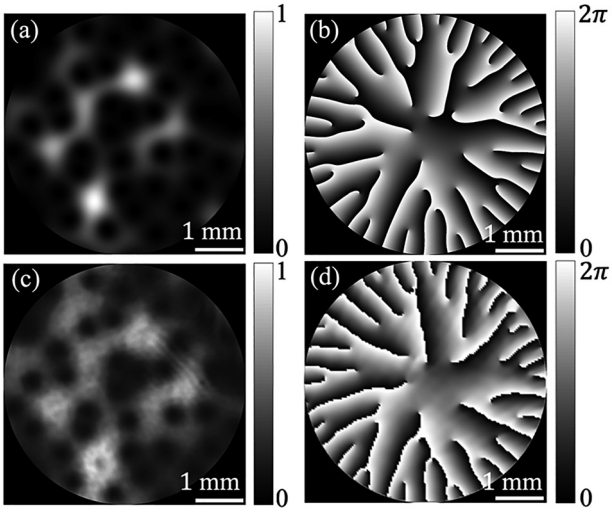

Figure 1: Theoretical results of the (a) intensity distribution and (b) phase distribution of one realization (instantaneous electric field). (c) and (d), the corresponding experimental results of the intensity distribution and phase distribution.

In practical circumstance, one could express the ensemble average as the summation of large number of random electric fields, to be a good approximation, if the random process is stationary, i.e.,

$$\langle T^*(\mathbf{r}_1)T(\mathbf{r}_2)\rangle=\frac{1}{N}\sum_{n=1}^{N}T_n^*(\mathbf{r}_1)T_n(\mathbf{r}_2), \quad (9)$$

where N is the number of realizations. Eqs. (7)–(9) provides an efficient way to experimentally synthesize the TGSM beams based on incoherent superposition of the random fluctuating fields. The modulation of the amplitude and phase of each realization can be realized with the help of particular optical devices, such as a spatial light modulator (SLM) or a digital mirror device (DMD). It is worth to note that one can conveniently control the strength of twist phase, i.e., twist factor, in the process of generating the random realizations $T_n(\mathbf{r})$ since the twist factor is contained in the kernel function $H(\mathbf{r}, \mathbf{v})$ shown in Eq. (6).

3 Experiment

3.1 Generation of a TGSM beam via random mode superposition

Part I of Figure 2 shows our experimental setup for generating the TGSM beam. A linearly polarized beam ($\lambda=532$ nm) emitting from a diode-pumped solid state (DPSS) laser is expanded by a beam

expander (BE) and reflected by a reflective mirror (RM_1). We note here that the DPSS laser used here is a single longitudinal mode and TEM_{00} transverse mode laser (Cobolt Samba 532 nm laser). The beam then goes towards a beam splitter (BS). The transmitted portion entering part II is used as a reference wave to measure the twist factor of the generated TGSM beam, which we will discuss in the next subsection. The reflected portion impinges on a phase-only spatial light modulator (SLM, Pluto-VIS, Holoeye) on which a computer-generated hologram (CGH) is loaded to modulate the amplitude and phase of the incident beam. Although the phase-only SLM can modulate only the phase of the incident light, several methods have been proposed to simultaneously encode the amplitude and the phase information on a phase-only CGH. Here, we adopt the method for synthesizing the CGH of type 3 described in Ref. [53]. The basic idea is as follows: we first write the phase-only CGH as the form $h(x,y) = \exp[i\psi(A,\phi)]$, where ψ is the function of the prescribed amplitude A and phase ϕ. Note that A and ϕ are the spatially dependent. The $h(x,y)$ function is then expanded in terms of Fourier series and is associated with the phase modulation $\psi(A,\phi) = f(A)\sin(\phi)$ with $f(A)$ being an unknown function. Finally, the function $f(A)$ is solved by the equation $J_1[f(A)] = 0.582A$. The inset (a) in Figure 2 illustrates the typical CGH associated with the blazed grating to generate the single realization of the field.

The modulated light reflects from the SLM and passes through the BS again, entering a $4f$ optical system consisting of lenses L_1 and L_2. The use of the $4f$ system is to filter out the unwanted diffraction order and background noise with the help of the CA_2 located in the rear focal plane of L_1, and to image the modulated beam with unit magnification. The imaging plane is regarded as the source plane of the generated TGSM beam. The intensity and phase distributions of an instantaneous electric field measured from experiment are shown in Figure 1(c) and (d), corresponding to the theoretical results shown in Figure 1(a) and (b). One can see that the generated instantaneous field agrees reasonably well with the prescribed one. Since the TGSM beam is the incoherent superposition of a large number of realizations (randomly fluctuating electric fields), $N = 5000$ CGHs encoded with the random complex fields is prepared in advance and is stored in computer memory. The SLM operates in such a manner that at each time step, the chronologically earliest CGH is removed from the SLM's screen and replaced by a new CGH. The SLM's screen plays 5000 CGHs in cycle with each CGH being equal displaying time; about 18 ms. The CCD captures the intensity distributions of all realizations. The average intensity distribution of the TGSM beam can be obtained by averaging over the intensity of all realizations. In the experiment, we generate two TGSM beams with twist factors $\mu_0 = 6.25\text{mm}^{-2}$ and $\mu_0 = -6.25\text{mm}^{-2}$. This can be done by preparing two sets of CGHs, one for 6.25mm^{-2} and the other for -6.25mm^{-2}.

Figure 3(a) and (i) illustrates the experimental results of the intensity distribution of the generated TGSM beams in the source plane with two different twist factors $\mu_0 = 6.25\text{mm}^{-2}$ and $\mu_0 = -6.25\text{mm}^{-2}$, respectively. The other beam parameters set in the CGH are $\sigma_0 = 1.6$ mm, $\delta_0 = 0.4$ mm. It is found that the two intensity distributions have the same Gaussian profile that is independent of the value of the twist factor. Nevertheless, the two TGSM beams exhibit different propagation characteristics if the circular symmetry of the beam is broken. In the experiment, we insert a thin lens L_3 with focal length $f = 200$ mm and a cylindrical lens (CL) with focal length $f_x = 150$ mm and $f_y = \infty$, and examine the intensity distributions at different propagation distances after two lenses. The experimental results are shown in Figure 3(a)–(h) and Figure 3(i)–(p). One can see that the rotation directions of the beam spot with respect to the propagation axis are opposite. The positive and negative twist factors correspond to the clockwise and counterclockwise rotating direction, respectively. However, such behavior allows one to judge only the sign of the twist factor. It is difficult to determine the magnitude of the twist factors quantitatively from the propagation intensity distributions.

3.2 Measurement of the twist factor

From Eq. (2), it is shown that the twist phase is contained in the phase of the two-point DOC function. To see clearly the role of the twist factor in the DOC, we write Eq. (2) as the more specific form, i.e.,

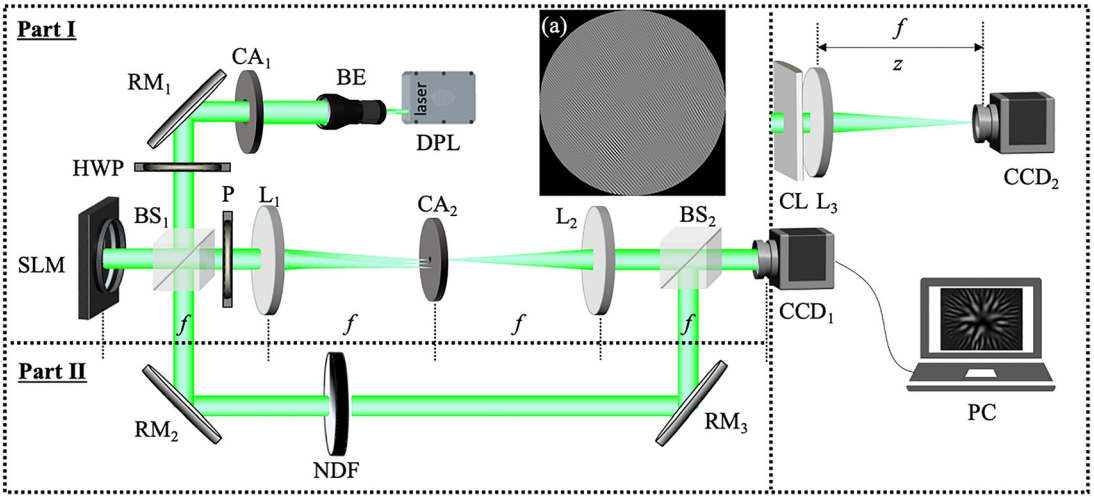

Figure 2: Experimental setup for synthesizing and measuring the TGSM beam with controllable twist phase. DPL, diode-pumped solid-state laser; BE, beam expander; CA_1, CA_2, circular apertures; RM_1, RM_2, RM_3, reflect mirrors; HWP, half-wave plate; BS_1, BS_2, beam splitters; SLM, spatial light modulator; P, linear polarizer; L_1, L_2, L_3, thin lenses; CL, cylindrical lens; NDF, neutral-density filter; PC, personal computers.

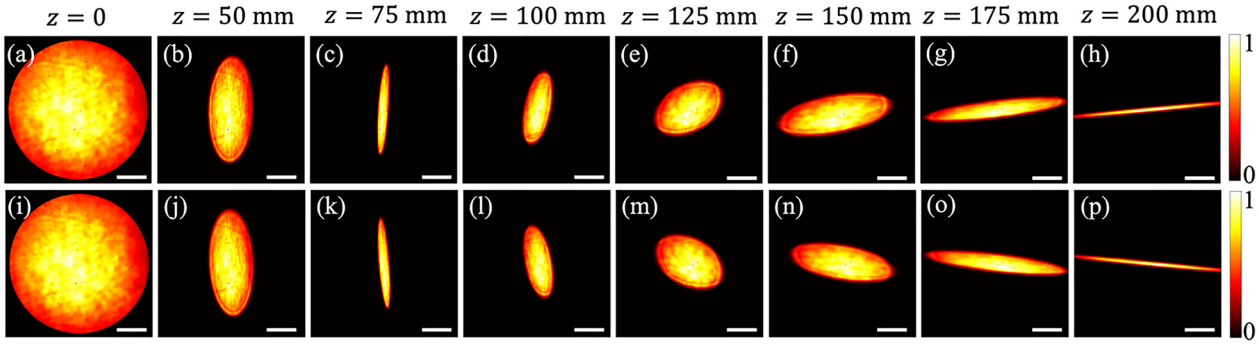

Figure 3: Experimental results of the normalized average intensity distributions of the generated TGSM source with $\mu_0 = 6.25\text{mm}^{-2}$ (top) and $\mu_0 = -6.25\text{mm}^{-2}$ (bottom), respectively, at different propagation distances. The scale bars in the figures are 1 mm.

$$\mu(\mathbf{r}_1, \mathbf{r}_2) = \exp\left[-\frac{1}{2\delta_0^2}|\mathbf{r}_1 - \mathbf{r}_2|^2\right] \times \{\cos[\mu_0(x_1y_2 - y_1x_2)] - i\sin[\mu_0(x_1y_2 - y_1x_2)]\}. \tag{10}$$

If we only concentrate on the real part of the DOC and fix the point $\mathbf{r}_2 = (x_2, y_2)$ as a reference point, in such a situation, the pattern of the real part looks like an interference pattern of two plane waves with its intensity truncated by a Gaussian profile. The period of the pattern turns out to be

$$T = \frac{2\pi}{\mu_0}\sqrt{\frac{1}{y_2^2} + \frac{1}{x_2^2}}. \tag{11}$$

Therefore, by measuring period of the pattern with a known reference point, one could determine the twist factor quantitatively, i.e., $\mu_0 = (2\pi/T)\sqrt{x_2^{-2} + y_2^{-2}}$.

The real part of the DOC can be measured by interferometry methods. Here, the generated TGSM beam obeys Gaussian statistics. Thus, its DOC can be measured with the help of the famous Hanbury Brown and Twiss (HBT) experiment. The HBT experiment, also known as the intensity correlation between two spatial points, is an efficient way to measure the DOC function of partially coherent light with Gaussian statistics [54–56]. The relation between the intensity correlation and the DOC is established via Gaussian momentum theorem [54], i.e.,

$$G(\mathbf{r}_1, \mathbf{r}_2) = \langle I(\mathbf{r}_1)I(\mathbf{r}_2)\rangle = S(\mathbf{r}_1)S(\mathbf{r}_2) + |W(\mathbf{r}_1, \mathbf{r}_2)|^2, \tag{12}$$

where $S(\mathbf{r}) = \langle I(\mathbf{r})\rangle$ is the average intensity of the light beam and $|W(\mathbf{r}_1, \mathbf{r}_2)|^2 = S(\mathbf{r}_1)S(\mathbf{r}_2)|\mu(\mathbf{r}_1, \mathbf{r}_2)|^2$. It indicates from Eq. (12) that the HBT experiment only measures the modulus of the DOC function. The phase information is lost. In order to recover the phase information or real part of the DOC function, we recently introduced the generalized HBT experiment [52]. In this method, a reference wave is used to interfere with the to-be-detect random field. As shown in part II of Figure 2, a reference beam transmitted from the BS passes the RM_2, neutral density filter (NDF), and RM_3, then, coaxially interferes with the generated TGSM beam. A CCD camera records a large number of instantaneous intensity distributions to calculate the intensity correlation function. In this case, the instantaneous mixed electric field can be written as

$$E_s(\mathbf{r}) = E(\mathbf{r}) + E_r(\mathbf{r}), \tag{13}$$

where E_s, E and E_r represent the mixed field, random field, and reference field, respectively. By applying the Gaussian momentum theorem, the intensity correlation of such mixed field turns out to be (after some mathematical manipulations)

$$\begin{aligned} G_s(\mathbf{r}_1, \mathbf{r}_2) &= \langle I_s(\mathbf{r}_1)I_s(\mathbf{r}_2)\rangle \\ &= S_s(\mathbf{r}_1)S_s(\mathbf{r}_2) + |W(\mathbf{r}_1, \mathbf{r}_2)|^2 \\ &\quad + 2\sqrt{S_r(\mathbf{r}_1)S_r(\mathbf{r}_2)}\,\text{Re}[W(\mathbf{r}_1, \mathbf{r}_2)], \end{aligned} \tag{14}$$

where I_s and $S_s = S(\mathbf{r}) + S_r(\mathbf{r})$, respectively, stand for the instantaneous intensity and the average intensity of the mixed field. $S_r(\mathbf{r})$ is the intensity distribution of the reference field. From Eq. (14), it is found that the last term of the right side contains the real part information of the CSD function. Combining Eqs. (1), (12) and (14), we finally obtain the expression

$$\text{Re}[\mu(\mathbf{r}_1, \mathbf{r}_2)] = \frac{G_s(\mathbf{r}_1, \mathbf{r}_2) - G(\mathbf{r}_1, \mathbf{r}_2) - \bar{S}(\mathbf{r}_1, \mathbf{r}_2)}{2\sqrt{S_r(\mathbf{r}_1)S_r(\mathbf{r}_2)S(\mathbf{r}_1)S(\mathbf{r}_2)}}, \tag{15}$$

where $\bar{S}(\mathbf{r}_1, \mathbf{r}_2) = S(\mathbf{r}_1)S_r(\mathbf{r}_2) + S_r(\mathbf{r}_1)S(\mathbf{r}_2) + S_r(\mathbf{r}_1)S_r(\mathbf{r}_2)$. From Eq. (15), one could extract the real part of the DOC function experimentally through the following procedures: First, the average intensity distribution of the reference field $S_r(\mathbf{r})$ and the random field $S(\mathbf{r})$ are measured, respectively. Second, the intensity correlations of the random field (the reference arm is closed) and the mixed field are measured, respectively. Finally, the real part of the DOC is evaluated by the measured quantities according to Eq. (15). In the experiment, the CCD records 5000 instantaneous intensity distributions of the random field and the mixed field to calculate the average intensity distribution and the intensity correlation.

Figure 4(a)–(d) present our experiment results of the real part of the DOC function of the generated TGSM beam in the source plane at four different reference points which are $\mathbf{r}_2$ = (0, 0), (0, σ_0), ($\sigma_0/\sqrt{2}, \sigma_0/\sqrt{2}$), and ($\sigma_0$, 0). For convenience of comparison, the corresponding theoretical results are shown in Figure 4(e)–(h). The measured beam width σ_0 is about 1.6 mm. It can be seen from Figure 4 that the real part of the DOC pattern is closely dependent on the specific reference point we choose. When $\mathbf{r}_2$ = (0, 0), the result reduces to a Gaussian profile that is $\text{Re}[\mu(\mathbf{r}_1, 0)] = \exp(-\mathbf{r}_1^2/2\delta_0^2)$. The value of beam width δ_0 is obtained through measuring the width of this profile. If the reference point leaves the coordinate origin, the real part of the DOC displays a clear interference pattern, as expected. The line direction of

pattern coincides with the radial direction in polar coordinate, whereas the period of the pattern is dependent on the position of reference point as shown in Eq. (11). Note that only a few interference fringes are visible, since the pattern is truncated by a Gaussian function. To determine the twist factor, we plot in Figure 5(a) and (b) the cross-line (red circular dots) of the real part of the DOC in Figure 5(a) at $y = \sigma_0$ and in Figure 5(b) at $x = \sigma_0$, respectively. By theoretically fitting the experimental data, we obtain that the twist factor is about 6.33 and 6.12 mm^{-2} in Figure 5(a) and (b), respectively, very closing to the theoretical set value 6.25 mm^{-2}. In addition, we also experimentally generate the TGSM beams with different twist factors and measure the twist factors (not shown here). The results show that the measured twist factors agree well with the theoretical setting values, demonstrating the reliability of our generation and measurement method.

It is known from Refs. [35, 57] that the amount of the time-average OAM flux of the TGSM beam along propagation direction is $J_z = -2\mu_0 k\sigma_0^2 \hbar$, where k is the wave number. The OAM flux of the TGSM beam is proportional to the twist factor and the square of the beam width. The beam width can be obtained simply from the measurement of the intensity profile of the beam simply. Hence, our method for measuring the twist factor is crucial to determine the OAM flux of the TGSM beam, paving the way to study the transfer of OAM with matter further.

4 Conclusions

In summary, we presented an effective way to synthesize the TGSM beam with the help of a single phase-only SLM. The methodology based on the incoherent superposition of random modes obeying Gaussian statistics is discussed. The key in our method is to simultaneously control the amplitude and phase of each random mode (realization) using the phase-only SLM. This allows one to generate the TGSM beams with controllable twist factor without changing the apparatus physically. We validate our method by experimentally generating the TGSM beams with reversed twist phases. The experimental results agree well with the theoretical predictions.

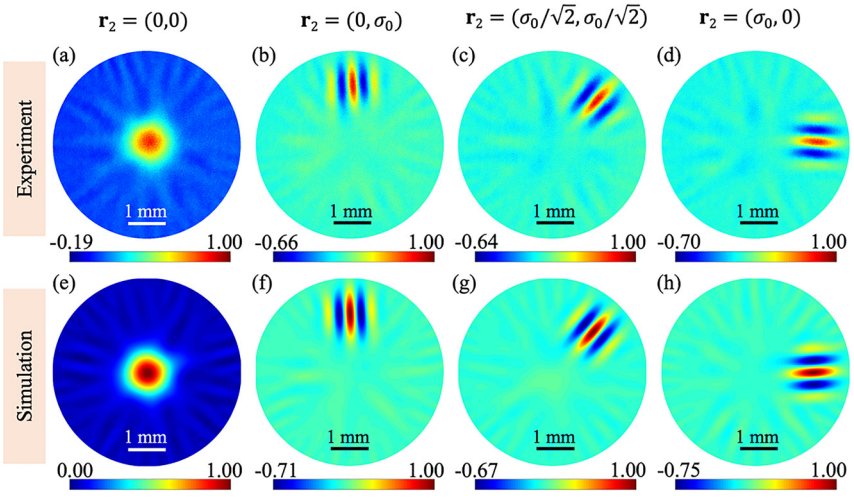

Figure 4: (a)–(d) Experimental and (e)–(h) simulation results of the real part of the DOC of the TGSM beam in the source plane with different reference points $\mathbf{r}_2$.

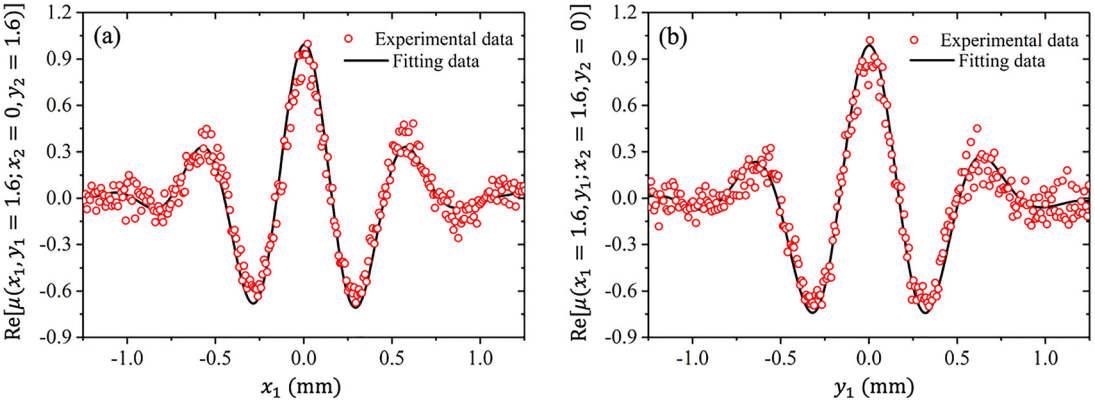

Figure 5: The cross-line of the real part of the DOC function of the TGSM beam when the reference points are selected as (a) $\mathbf{r}_2 = (0, \sigma_0)$ and (b) $\mathbf{r}_2 = (\sigma_0, 0)$. The solid curves denote the theoretical fits from the experimental results.

Furthermore, we proposed a reliable protocol to quantitively determine the twist factor of the TGSM beam. The kernel of our protocol is to acquire the real part of the DOC from the measurement of the intensity correlations of the mixed fields form by the superposition of a reference wave and the generated random TGSM beam. The twist factor is extracted through evaluating the period of the interference pattern in the real part of the DOC. Our results provide a convenient way to control and detect the second-order phase of a partially coherent light field that are expected to find uses in novel optical imaging based on the coherence phase modulation.

Author contributions: All the authors have accepted responsibility for the entire content of this submitted manuscript and approved submission.

Research funding: This work was supported by the National Key Research and Development Project of China (Grant No. 2019YFA0705000), the National Natural Science Foundation of China (NSFC) (Grant Nos. 91750201, 11774251, 11874046, 11974218, 11904247, 12104263 and 12174279), the Innovation Group of Jinan (Grant No. 2018GXRC010), the Natural Science Foundation of the Jiangsu Higher Education Institutions of China (Grant No. 19KJB140017), the China Postdoctoral Science Foundation (Grant No. 2019M661915), the Natural Science Foundation of Shandong Province (Grant No. ZR2019 QA004), the Priority Academic Program Development of Jiangsu Higher Education Institutions, the Qing Lan Project of Jiangsu Province of China, the Local Science and Technology Development Project of the Central Government (Grant No. YDZX20203700001766) and the Postgraduate Research & Practice Innovation Program of Jiangsu Province (Grant No. KYCX21_2935).

Conflict of interest statement: The authors declare no conflicts of interest regarding this article.

References

[1] M. J. Padgett, "Orbital angular momentum 25 years on [Invited]," *Opt. Express*, vol. 25, no. 10, pp. 11265–11274, 2017.
[2] S. Fu, Y. Zhai, J. Zhang, et al., "Universal orbital angular momentum spectrum analyzer for beams," *PhotoniX*, vol. 1, 2020, Art no. 19.
[3] Y. Shen, X. Wang, Z. Xie, et al., "Optical vortices 30 years on: OAM manipulation from topological charge to multiple singularities," *Light Sci. Appl.*, vol. 8, p. 90, 2019.
[4] Y. Chen, W. Shen, Z. Li, et al., "Underwater transmission of high-dimensional twisted photons over 55 meters," *PhotoniX*, vol. 1, 2020, Art no. 5.
[5] L. Allen, M. W. Beijersbergen, R. J. C. Spreeuw, et al., "Orbital angular momentum of light and the transformation of Laguerre-Gaussian laser modes," *Phys. Rev. A*, vol. 45, no. 11, pp. 8185–8189, 1992.
[6] G. Gbur, *Singular Optics*, Los Angeles, CRC Press, 2017.
[7] X. Wang, Z. Nie, Y. Liang, et al., "Recent advances on optical vortex generation," *Nanophotonics*, vol. 7, no. 9, pp. 1533–1556, 2018.
[8] H. Wang, L. Liu, C. Zhou, et al., "Vortex beam generation with variable topological charge based on a spiral slit," *Nanophotonics*, vol. 8, no. 2, pp. 317–324, 2019.
[9] Z. Qiao, Z. Wan, G. Xie, et al., "Multi-vortex laser enabling spatial and temporal encoding," *PhotoniX*, vol. 1, 2020, Art no. 13.
[10] D. P. Ghai, P. Senthilkumaran, and R. S. Sirohi, "Single-slit diffraction of an optical beam with phase singularity," *Opt. Laser. Eng.*, vol. 47, no. 1, pp. 123–126, 2009.
[11] H. Zhou, L. Shi, X. Zhang, et al., "Dynamic interferometry measurement of orbital angular momentum of light," *Opt. Lett.*, vol. 39, no. 20, pp. 6058–6061, 2014.
[12] Y. Yang, X. Zhu, J. Zeng, et al., "Anomalous bessel vortex beam: modulating orbital angular momentum with propagation," *Nanophotonics*, vol. 7, no. 3, pp. 677–682, 2018.
[13] W. C. Soares and S. Chávez-Cerda, "Unveiling a truncated optical lattice associated with a triangular aperture using light's orbital angular momentum," *Phys. Rev. Lett.*, vol. 105, no. 5, 2010, Art no. 053904.
[14] K. Dai, C. Gao, L. Zhong, et al., "Measuring OAM states of light beams with gradually changing-period gratings," *Opt. Lett.*, vol. 40, no. 4, pp. 562–565, 2015.
[15] G. G. Berkhout, M. J. Lavery, J. Courtial, et al., "Efficient sorting of orbital angular momentum states of light," *Phys. Rev. Lett.*, vol. 105, no. 15, 2010, Art no. 153601.
[16] J. Zhou, Wu. Zhang, and L. Chen, "Experimental detection of high-order or fractional orbital angular momentum of light based on a robust mode converter," *Appl. Phys. Lett.*, vol. 108, no. 11, 2016, Art no. 111108.
[17] S. N. Alperin, R. D. Niederriter, J. T. Gopinath, et al., "Quantitative measurement of the orbital angular momentum of light with a single, stationary lens," *Opt. Lett.*, vol. 41, no. 21, pp. 5019–5022, 2016.
[18] D. M. Palacios, I. D. Maleev, A. S. Marathay, et al., "Spatial correlation singularity of a vortex field," *Phys. Rev. Lett.*, vol. 92, 2004, Art no. 143905.
[19] C. Zhao, F. Wang, Y. Dong, et al., "Effect of spatial coherence on determining the topological charge of a vortex beam," *Appl. Phys. Lett.*, vol. 101, 2012, Art no. 261104.
[20] X. Liu, J. Zeng, and Y. Cai, "Review on vortex beams with low spatial coherence," *Adv. Phys. X*, vol. 4, 2019, Art no. 1626766.
[21] M. Dong, C. Zhao, Y. Cai, et al., "Partially coherent vortex beams: fundamentals and applications," *Sci. China Phys. Mech. Astron.*, vol. 64, 2021, Art no. 224201.
[22] J. Courtial, K. Dholakia, L. Allen, et al., "Gaussian beams with very high orbital angular momentum," *Opt. Commun.*, vol. 144, nos 4–6, pp. 210–213, 1997.
[23] V. V. Kotlyar, A. A. Kovalev, and A. P. Porfirev, "Astigmatic laser beams with a large orbital angular momentum," *Opt. Express*, vol. 26, no. 1, pp. 141–156, 2018.
[24] R. Simon and N. Mukunda, "Twisted Gaussian schell-model beams," *J. Opt. Soc. Am. A*, vol. 10, no. 9, pp. 95–109, 1993.
[25] J. Serna and J. M. Movilla, "Orbital angular momentum of partially coherent beams," *Opt. Lett.*, vol. 26, no. 7, pp. 405–407, 2001.

[26] G. Gbur, "Partially coherent beam propagation in atmospheric turbulence," *J. Opt. Soc. Am. A*, vol. 31, pp. 2038–2045, 2014.
[27] X. Lu, Y. Shao, C. Zhao, et al., "Noniterative spatially partially coherent diffractive imaging using pinhole array mask," *Adv. Photon.*, vol. 1, 2019, Art no. 016005.
[28] Y. Shen, H. Sun, D. Peng, et al., "Optical image reconstruction in 4f imaging system: role of spatial coherence structure engineering," *Appl. Phys. Lett.*, vol. 118, 2021, Art no. 181102.
[29] D. Peng, Z. Huang, Y. Liu, et al., "Optical coherence encryption with structured random light," *PhotoniX*, vol. 2, 2021, Art no. 6.
[30] Y. Cai, Q. Lin, and D. Ge, "Propagation of partially coherent twisted anisotropic Gaussian Schell-model beams in dispersive and absorbing media," *J. Opt. Soc. Am. A*, vol. 19, no. 10, pp. 2036–2042, 2002.
[31] M. A. Shukri, A. A. Alkelly, and Y. S. Alarify, "Spatial correlation properties of twisted partially coherent light focused by diffractive axicons," *J. Opt. Soc. Am. A*, vol. 29, no. 9, pp. 2019–2027, 2012.
[32] Y. Cai and S. Zhu, "Orbital angular moment of a partially coherent beam propagating through an astigmatic ABCD optical system with loss and gain," *Opt. Lett.*, vol. 39, pp. 1968–1971, 2014.
[33] W. Fu and P. Cao, "Second-order statistics of a radially polarized partially coherent twisted beam in a uniaxial crystal," *J. Opt. Soc. Am. A*, vol. 34, no. 9, pp. 1703–1710, 2017.
[34] L. Liu, Y. Chen, L. Guo, et al., "Twist phase-induced changes of the statistical properties of a stochastic electromagnetic beam propagating in a uniaxial crystal," *Opt. Express*, vol. 23, no. 9, pp. 12454–12467, 2015.
[35] X. Peng, L. Liu, F. Wang, et al., "Twisted Laguerre-Gaussian Schell-model beam and its orbital angular moment," *Opt. Express*, vol. 26, no. 26, pp. 33956–33969, 2018.
[36] R. Borghi, F. Gori, G. Guattari, et al., "Twisted Schell-model beams with axial symmetry," *Opt. Lett.*, vol. 40, no. 19, pp. 4504–4507, 2015.
[37] R. Borghi, "Twisting partially coherent light," *Opt. Lett.*, vol. 43, no. 8, pp. 1627–1630, 2018.
[38] Z. Mei and O. Korotkova, "Random sources for rotating spectral densities," *Opt. Lett.*, vol. 42, no. 2, pp. 255–258, 2017.
[39] F. Gori and M. Santarsiero, "Devising genuine spatial correlation functions," *Opt. Lett.*, vol. 32, no. 24, pp. 3531–3533, 2007.
[40] F. Gori and M. Santarsiero, "Devising genuine twisted cross-spectral densities," *Opt. Lett.*, vol. 43, no. 3, pp. 595–598, 2018.
[41] Z. Tong and O. Korotkova, "Beyond the classical Rayleigh limit with twisted light," *Opt. Lett.*, vol. 37, no. 13, pp. 2595–2597, 2012.
[42] C. Zhao, Y. Cai, and O. Korotkova, "Radiation force of scalar and electromagnetic twisted Gaussian Schell-model beams," *Opt. Express*, vol. 17, no. 24, pp. 21472–21487, 2009.
[43] F. Wang, Y. Cai, H. T. Eyyuboglu, et al., "Twist phase-induced reduction in scintillation of a partially coherent beam in turbulent atmosphere," *Opt. Lett.*, vol. 37, no. 2, pp. 184–186, 2012.
[44] X. Peng, H. Wang, L. Liu, et al., "Self-reconstruction of twisted Laguerre-Gaussian Schell-model beams partially blocked by an opaque obstacle," *Opt. Express*, vol. 28, pp. 31510–31523, 2020.
[45] A. T. Friberg, B. Tervonen, and J. Turunen, "Interpretation and experimental demonstration of twisted Gaussian Schell-model beams," *J. Opt. Soc. Am. A*, vol. 11, no. 6, pp. 1818–1826, 1994.
[46] H. Wang, X. Peng, L. Liu, et al., "Generating bona fide twisted Gaussian Schell-model beams," *Opt. Lett.*, vol. 44, no. 15, pp. 3709–3712, 2019.
[47] C. Tian, S. Zhu, H. Huang, et al., "Customizing twisted Schell-model beams," *Opt. Lett.*, vol. 45, no. 20, pp. 5880–5883, 2020.
[48] D. Ambrosini, V. Bagini, F. Gori, et al., "Twisted Gaussian schell-model beams: a superposition model," *J. Mod. Opt.*, vol. 41, no. 7, pp. 1391–1399, 1994.
[49] Y. Cai, Q. Lin, and O. Korotkova, "Ghost imaging with twisted Gaussian Schell-model beam," *Opt. Express*, vol. 17, pp. 2453–2464, 2009.
[50] Y. Liu, X. Liu, L. Liu, et al., "Ghost imaging with a partially coherent beam carrying twist phase in a turbulent ocean: a numerical approach," *Appl. Sci.*, vol. 8, no. 3023, 2019, https://doi.org/10.3390/app9153023.
[51] M. W. Hyde, "Stochastic complex transmittance screens for synthesizing general partially coherent sources," *J. Opt. Soc. Am. A*, vol. 37, no. 2, pp. 257–264, 2020.
[52] Z. Huang, Y. Chen, F. Wang, et al., "Measuring complex degree of coherence of random light fields with generalized Hanbury Brown-Twiss experiment," *Phys. Rev. Appl.*, vol. 13, no. 4, 2020, Art no. 044020.
[53] A. Victor, R. Ulises, C. Rosibel, et al., "Pixelated phase computer holograms for the accurate encoding of scalar complex fields," *J. Opt. Soc. Am. A*, vol. 24, no. 11, pp. 3500–3507, 2007.
[54] L. Mandel and E. Wolf, *Optical Coherence and Quantum Optics*, Cambridge, Cambridge University, 1995.
[55] T. Hassinen, J. Tervo, T. Setälä, et al., "Hanbury Brown-Twiss effect with electromagnetic waves," *Opt. Express*, vol. 19, no. 16, pp. 15188–15195, 2011.
[56] J. W. Goodman, *Statistical Optics*, New York, John Wiley & Sons, 1985.
[57] L. Liu, Y. Huang, Y. Chen, et al., "Orbital angular moment of an electromagnetic Gaussian Schell-model beam with a twist phase," *Opt. Express*, vol. 23, no. 23, pp. 30283–30296, 2015.